

Accepted Manuscript

Title: Application of a novel respirometric methodology to characterize mass transfer and activity of H₂S-oxidizing biofilms in biotrickling filter beds

Author: Wenceslao Bonilla-Blancas Mabel Mora Sergio Revah Juan Antonio Baeza Javier Lafuente Xavier Gamisans David Gabriel Armando González-Sánchez



PII: S1369-703X(15)00075-3
DOI: <http://dx.doi.org/doi:10.1016/j.bej.2015.02.030>
Reference: BEJ 6142

To appear in: *Biochemical Engineering Journal*

Received date: 24-5-2014
Revised date: 17-2-2015
Accepted date: 26-2-2015

Please cite this article as: Wenceslao Bonilla-Blancas, Mabel Mora, Sergio Revah, Juan Antonio Baeza, Javier Lafuente, Xavier Gamisans, David Gabriel, Armando González-Sánchez, Application of a novel respirometric methodology to characterize mass transfer and activity of H₂S-oxidizing biofilms in biotrickling filter beds, *Biochemical Engineering Journal* <http://dx.doi.org/10.1016/j.bej.2015.02.030>

This is a PDF file of an unedited manuscript that has been accepted for publication. As a service to our customers we are providing this early version of the manuscript. The manuscript will undergo copyediting, typesetting, and review of the resulting proof before it is published in its final form. Please note that during the production process errors may be discovered which could affect the content, and all legal disclaimers that apply to the journal pertain.

Application of a novel respirometric methodology to characterize mass transfer and activity of H₂S-oxidizing biofilms in biotrickling filter beds

Wenceslao Bonilla-Blancas^{a,c,e}, Mabel Mora^a, Sergio Revah^b, Juan Antonio Baeza^a, Javier Lafuente^a, Xavier Gamisans^d, David Gabriel^a, Armando González-Sánchez^{c*}

^aGENOCOV, Departament d'Enginyeria Química. Universitat Autònoma de Barcelona. Edifici Q. Campus de Bellaterra. 08193 Bellaterra, Barcelona, Spain.

^bDepartamento de Procesos y Tecnología, Universidad Autónoma Metropolitana Cuajimalpa, México D.F., Mexico.

^cInstituto de Ingeniería, Universidad Nacional Autónoma de México, Ciudad Universitaria, México D.F., Mexico.

^dDepartament d'Enginyeria Minera i Recursos Naturals, Universitat Politècnica de Catalunya, Bases de Manresa 61-73, 08240 Manresa, Spain.

^eTecnológico de Estudios Superiores de Ecatepec, Ecatepec de Morelos, Mexico.

* Corresponding author: Coordination of Environmental Engineering, Building 5, 2nd Floor, Office 312, Engineering Institute UNAM, Circuito Escolar, Ciudad Universitaria, ZIP 04510 Mexico D.F., Mexico. Tel.: + (52) 55 56 23 36 00 x8711

agonzalezs@iingen.unam.mx

1 Highlights

2

- 3 • A novel respirometer design characterized the kinetics in H₂S-oxidizing biofilms
- 4 • H₂S biofiltration properties were evaluated from a sample of biotrickling filter bed
- 5 • Short-term respirometric assays (< 20 min) were performed
- 6 • A mathematical model of the biotrickling filter bed respirometry was developed
- 7 • The non-wetted biofilm fraction contributed 65% to the overall removal of H₂S

1 ABSTRACT

2 The elimination capacity of gaseous H₂S biofiltration can be limited either by mass transfer or
3 bioreaction in the biofilm. Assessment of the biological activity of immobilized cells (biofilm)
4 usually implies morphological and physiological changes during the adaptation of cells to
5 respirometric devices operated as suspended cultures. In this study, respirometry of
6 heterogeneous media is advised as a valuable technique for characterizing mass transport and
7 biological activity of H₂S-oxidizing biofilms attached on two packing materials from operative
8 biotrickling filters. Controlled flows of liquid and H₂S-containing air were recirculated through
9 a closed heterogeneous respirometer allowing a more realistic estimation of the biofilm activity
10 by the experimental evaluation of the oxygen uptake rate (OUR). Specific maximum OUR of
11 23.0 and 38.5 mmol O₂ (g biomass min)⁻¹ were obtained for Pall Rings and Polyurethane Foam,
12 respectively. A mathematical model for the determination of kinetic-related parameters such as
13 the maximum H₂S elimination capacity and morphological properties of biofilm (i.e. thickness
14 and fraction of wetted area of packing bed) was developed and calibrated. With the set of
15 parameters obtained, the external oxygen mass transport to the wetted biofilm was found to
16 limit the global H₂S biofiltration capacity, whereas the non-wetted biofilm was the dominant
17 route for the gaseous O₂ and H₂S mass transfer to the biofilm. Oxygen diffusion rate was the
18 limiting step in the case of very active biofilms.

19 KEYWORDS

20 *OUR*; Hydrogen sulfide; heterogeneous respirometry; wetted/non-wetted biofilm; mathematical
21 model; mass transfer.

1

2 **1. INTRODUCTION**

3 Hydrogen sulfide (H₂S) is a volatile inorganic compound commonly found in waste gas
4 streams (e.g. biogas from landfills and wastewater treatment plants), with a typical composition
5 ranging from 0.0002 % to 2.0% [1-2]. Biofilters (BF) and biotrickling filters (BTF) have been
6 widely studied and applied by several research groups and companies to desulfurize polluted,
7 odorous air or energetic gases such as biogas [3-4]. Therefore, the application of these
8 technologies avoids the emission of harmful gases and odors, which cause human hazard risks
9 and also corrosion damages on cogeneration engines in case of recovering energy from H₂S
10 containing waste gases.

11 Several parameters can be monitored and controlled during waste gas biofiltration, such as inlet
12 and outlet gaseous pollutant concentrations or flow rates, which allow calculating the overall
13 removal efficiency. However, biodegradation kinetics are usually difficult to determine [5].
14 Respirometry consists on the measurement and interpretation of the biological oxygen
15 consumption rate under well-defined experimental conditions and is a typical tool to assess the
16 degradation activity of microbial cultures [6-7]. The performance of this assay has been
17 traditionally used with suspended cells [8-9], namely Suspended Culture Respirometry (SCR),
18 which implies biofilm destruction when it is applied to monitor biological activity of
19 immobilized biomass. In SCR the original physiology of cells, as well as the mass transport
20 phenomena occurring in the biofilm, are not considered which drives to an overestimated
21 biological activity [10]. A realistic assessment of the biodegradation activity measured from a
22 sample of colonized packed bed would allow improving the strategies to adequately operate
23 and control biofilters.

1 Some adapted respirometric methodologies to study biodegradation kinetics of immobilized
2 biomass have been already proposed. In this sense, preliminary studies have been performed
3 towards the application of heterogeneous respirometry (HR) to characterize H₂S-oxidizing
4 biofilms [5, 11]. However, in these methodologies the liquid and/or gas phases remained static
5 [12-13], which do not simulate properly the dynamic nature of the flowing phases of a BF or
6 BTF and, in consequence, altered the real biofilm conditions during tests. The effect of external
7 mass transfer resistance on the H₂S elimination seems to be significant for the performance of
8 BFs and BTFs, and especially in aerobic systems where the mass transport of gaseous oxygen
9 to the biofilm could limit the global process [14]. Instead, the HR is a novel methodology based
10 on the measurement of the biological activity of immobilized biomass with a minimum
11 handling and damaging of the biofilm associated. HR also reproduces the dynamic conditions
12 of the flowing phases. In addition, in the abovementioned studies only the pollutant
13 concentration in the gas-phase has been monitored [15], while the oxygen concentration in the
14 gas phase was not analyzed. The latter is a critical variable that defines the H₂S biological
15 oxidation. Overall, the HR technique has not been extensively applied yet and requires further
16 experimental and modeling research in order to be improved.

17 Thus, the aim of this work was to apply, assess and improve the HR methodology to
18 characterize H₂S-oxidizing activity and mass transport phenomena of specialized biofilms
19 grown on packed beds of desulfurizing BTFs. Complementary, a mathematical model is
20 developed and calibrated to describe the process and the intrinsic oxygen uptake rates (OUR)
21 induced by the oxidation of H₂S in the biofilm. The mathematical model considers both wetted
22 and non-wetted biofilm surfaces of the packing material. Experimental data of oxygen profiles
23 in the gas and the liquid phase together with the application of the mathematical model allowed

1 estimating the maximum H₂S elimination capacity of the packing materials. Although no
2 experimental data was available from inside the biofilm, the model was used to theoretically
3 identify and assess the potential limiting steps in H₂S bio-oxidation.

4 **2. MATERIALS AND METHODS**

5 **2.1. Heterogeneous respirometer setup**

6 The experimental system consisted of a transparent PVC cylindrical BTF, with an internal
7 diameter of 0.06 m and a height of 0.50 m. The packed bed height filled with random packing
8 was 0.26 m (a working volume of 0.73 L). In Fig. 1 a schematic of the HR is presented. During
9 respirometric assays the liquid phase was continuously recirculated at a flow rate of $2.25 \cdot 10^{-2}$
10 $\text{m}^3 \text{h}^{-1}$ with a peristaltic pump (77200-12, Cole Parmer, USA) while the gas phase was counter-
11 currently recirculated with a gas compressor (Model 3112, Boxer, England) at $0.09 \text{m}^3 \text{h}^{-1}$.

Here Figure 1.

12

13

14 The HR was provided with an oxygen gas analyzer (SIDOR module OXOR-P, SICK,
15 Germany) and also with a galvanic dissolved oxygen sensor (CellOx 325, WTW, Germany)
16 connected to a bench top meter (Inolab Terminal level 3, WTW, Germany) to monitor the
17 oxygen concentration in each phase. The pH was monitored in-situ (Sentix 20, WTW,
18 Germany) and accurately controlled at 7.0 ± 0.1 by a high precision two-channel micro-burette
19 (Multi burette 2S, Crison, USA) by 1M HCl and 1M NaOH addition. Sensors data were
20 continuously recorded in a personal computer with software developed for process monitoring

1 and control with NI LabWindows CVI. Temperature was not directly controlled in the HR.
2 Instead, room temperature was kept constant at 21°C.

3

4 **2.2. H₂S-oxidizing immobilized biomass**

5 Two desulfurizing BTFs with different packing material, polyurethane foam cubes (EDT,
6 Eckenhaid-Eckental, Germany) and stainless steel pall rings (KEVINCPP, Mumbai, India),
7 namely PUF and PR, respectively, were used in this study (Table SM1, Supplementary
8 Material). The BTFs were inoculated with activated sludge from a municipal wastewater
9 treatment plant to obtain an enriched neutrophilic H₂S-oxidizing consortium. Initially, the
10 inoculum was circulated through the packing material during 8h without liquid renewal and
11 with a counter-current aeration flow of 0.03 m³·h⁻¹. Afterwards, the BTF was fed during 2
12 months with a constant H₂S inlet concentration of 300 ppm_v while setting the empty bed
13 residence time (EBRT) to 30 s (48 g S m⁻³ h⁻¹). The pH was monitored and automatically
14 controlled to 7.0. The composition of the mineral medium used to grow up the immobilized
15 culture contained (g L⁻¹): NH₄Cl, (1); KH₂PO₄, (0.12); K₂HPO₄, (0.15); CaCl₂, (0.02);
16 MgSO₄·7H₂O, (0.2); and trace elements, 1 mL L⁻¹ [4]. Additionally, bicarbonate was added as
17 the microbial carbon source to the mineral medium (3.5 g L⁻¹ NaHCO₃).

18

19 **2.3. Experimental approach of the heterogeneous respirometry**

20 Abiotic and biotic experiments were performed to characterize the mass transfer phenomena
21 and the H₂S-oxidizing activity of the biofilm. First, several abiotic assays were performed at
22 different gas and liquid linear velocities with two types of packing material (PUF and PR) to
23 estimate the overall volumetric mass transfer coefficient ($K_{La_{g-l}}$) corresponding to oxygen. The
24 procedure to obtain the experimental data was applied as follows. The BTF was filled with

1 sterilized packing material followed by the addition of mineral medium (126 mL). The gas and
2 liquid phases were counter-currently circulated while all oxygen was stripped out from the HR
3 by feeding nitrogen gas at a flow of $0.03 \text{ m}^3 \cdot \text{h}^{-1}$. Once the oxygen was absent, a controlled air
4 flow ($0.03 \text{ m}^3 \cdot \text{h}^{-1}$) was fed to the HR generating different time-dependent oxygen concentration
5 profiles in both phases. Different velocities for gas (43.4; 57.8; 77.1; 101.2 m h^{-1}) and liquid
6 (6.9; 8.3; 10.8 m h^{-1} , respectively) were applied to assess the mass transfer phenomena in the
7 BTF. The liquid was assumed to be pure water due to the low salt content. Then, no ionic
8 effects were considered over oxygen transfer. Gaseous and dissolved oxygen profiles arising
9 from the abiotic assays were used to estimate the corresponding $K_L a_{g-l}$.

10 For the biotic assays, colonized packing material was withdrawn from the BTFs packed with
11 PUF and PR, respectively. The experimental test started with the addition of 126 mL of mineral
12 medium into the HR, which was continuously recirculated and aerated for some hours in order
13 to stabilize the biofilm and to allow exhausting the bioavailable substrates that could have
14 accumulated in the biofilm during the BTF operation (mainly H_2S). Afterwards, the HR was
15 closed and, while both phases were continuously recirculated, a pulse of gaseous pure H_2S (10
16 mL) was immediately injected in the gas phase to attain computed equilibrium concentrations
17 of 0.62 mmol L^{-1} (19.8 g m^{-3}) and 0.63 % (vol) in the liquid and gas phases, respectively. The
18 measurement of the equilibrium concentration into the liquid phase was theoretically calculated
19 using the corresponding Henry's constant for H_2S ($H_e=0.41$ [16]). Gas and liquid phases were
20 circulated at linear velocities of 101.2 and 10.8 m h^{-1} , respectively, and the oxygen
21 concentration evolution was continuously monitored in both phases. The abiotic and biotic
22 assays were performed by triplicate and once (H_2S consecutive additions affected the biofilm
23 physiology) respectively. Experimental conditions in terms of substrate, electron acceptor and
24 biomass concentrations must be those that allow *OUR* to be sensitive enough to produce a short

1 test (to avoid large biomass growth) with reduced uncertainty due to noise of measurements.
2 Large substrate concentrations in the gas phase are important since produce significant
3 variations of oxygen both in the gas and in the liquid phase. The latter is particularly important
4 when activity tests are combined with modeling to determine model parameters or to predict
5 system performance.

6

7 **2.4. Experimental determinations in the packed bed**

8 The amount of biomass attached to the packing support was quantified as follows [17]. Once
9 the corresponding assay was finished, the liquid pump was stopped and the packing material
10 was immediately weighted (W_1). After draining the liquid for a period of 30 minutes, the
11 support was weighted again (W_2). The weight difference between W_2 and W_1 was used to
12 determine the static hold-up which, together with the dynamic hold-up, was used to estimate
13 the volume fraction occupied by the liquid (ϵ_l^{Bed}). Once drained, the packing material was
14 carefully squeezed and/or shaken to withdraw all the biofilm and suspend it in a known amount
15 of water. The clean packing was dried for 12 hours in an oven at 50 °C to determine the weight
16 of the support (W_3). The suspended biomass was later centrifuged at 5000 rpm for 10 minutes
17 and the supernatant was discarded to determine the weight of wet biomass (W_4). The volume
18 fraction occupied by the biofilm (ϵ_b^{Bed}) was calculated dividing W_4 by the product of wet
19 biofilm density times the volume of the packing material tested. A wet biofilm density of 1.11 g
20 mL⁻¹ reported by Hugler et al. [18] for a similar biofilm was used to calculate ϵ_b^{Bed} . Finally,
21 the wet biomass was dried for 12 hours at 50 °C to determine the dry weight of the biomass
22 (W_5). The volume fraction occupied by the gas (ϵ_g^{Bed}) in the packed bed was also determined

1 taking into account the space occupied by the abovementioned fractions of the packed bed,
2 including the empty bed fraction of the packing material reported by the manufacturer (see
3 Table 1).

4

5 **2.5. Mathematical model development**

6 Mass balances for oxygen and H₂S in the gas, liquid and biofilm phases of the HR were stated
7 in Eqs. (1-6) based on the modeling approach by González-Sánchez et al. [19]. Due to bench
8 size and the batch operating mode of the HR, an ideally mixed regime was assumed for both
9 bulk phases. The reaction was considered to occur entirely in the biofilm since there was no
10 suspended biomass in the liquid phase either at the beginning or at the end of the assays. The
11 reaction considered in this study is a biological reaction being the catalyzer the biomass itself.
12 Free volumes of gas in the upper and lower sections of the HR and the liquid reservoir (see Fig.
13 1) were also considered in mass balances. As a particular assumption associated with the
14 operation mode and size of the experimental system, no axial concentration gradients were
15 considered due to the continuous recirculation of gas and liquid phases. The mechanism
16 proposed for H₂S removal in the BTF is shown in Fig. 2. Both wetted and non-wetted portions
17 of the biofilm were included in the model. As a common assumption often made in biofiltration
18 modeling, mass transfer resistance in the gas boundary layer over the wetted and non-wetted
19 biofilm was assumed negligible. More detailed model assumptions can be found elsewhere [5,
20 20].

Here Figure 2.

21

22 **2.5.1 Mass balance for the gas phase.**

1 In the packed bed

$$\frac{dC_{g,i}^{Bed}}{dt} = \frac{Q_g}{V_{Bed} \cdot \epsilon_g^{Bed}} (C_{g,i}^{Free} - C_{g,i}^{Bed}) - \frac{K_L \cdot a_{g-l}}{\epsilon_g^{Bed}} \cdot \left(\frac{C_{g,i}^{Bed}}{He_i} - C_{l,i}^{Bed} \right) - \frac{K_B \cdot a_{g-b}}{\epsilon_g^{Bed}} \cdot \left(\frac{C_{g,i}^{Bed}}{He_i} - C_{b-NW,i} \right) \quad (1)$$

2 with initial condition:

$$3 \quad t=0 \quad C_{g,i}^{Bed} = C_{g,i}^0$$

4 In the gaseous reservoir

$$\frac{dC_{g,i}^{Free}}{dt} = \frac{Q_g}{V_{g,i}^{Free}} (C_{g,i}^{Bed} - C_{g,i}^{Free}) \quad (2)$$

5 with initial condition:

$$6 \quad t=0 \quad C_{g,i}^{Free} = C_{g,i}^0$$

7 The subscript i refers to oxygen or H_2S , the two different gaseous compounds considered in the
8 mass balance.

9

10 **2.5.2. Mass balance for the liquid phase.**

11 In the packed bed

$$\frac{dC_{l,i}^{Bed}}{dt} = \frac{Q_l}{V_l^{Bed}} (C_{l,i}^{Res} - C_{l,i}^{Bed}) + \frac{K_L a_{g-l}}{\epsilon_l^{Bed}} \left(\frac{C_{g,i}^{Bed}}{He_i} - C_{l,i}^{Bed} \right) - \frac{K_B \cdot a_{l-b}}{\epsilon_l^{Bed}} (C_{l,i}^{Bed} - C_{b,i}) \quad (3)$$

12 with initial condition:

$$13 \quad t=0 \quad C_{l,i}^{Bed} = C_{l,i}^0$$

14 In the liquid reservoir

$$\frac{dC_{l,i}^{Res}}{dt} = \frac{Q_l}{V_l^{Res}} (C_{l,i}^{Bed} - C_{l,i}^{Res}) \quad (4)$$

1 with initial condition:

$$2 \quad t=0 \quad C_{l,i}^{Res} = C_{l,i}^0$$

3 **2.5.3. Mass balance for the biofilm**

Wetted biofilm

$$\frac{\partial C_{b,i}}{\partial t} = D_{eff,i} \frac{\partial^2 C_{b,i}}{\partial x^2} - r_{b,i} - OUR_{end} \quad (5)$$

with boundary conditions:

$$t=0; C_{b,i} = C_{b,i}^0$$

$$x=0; C_{b,i} = C_{l,i}$$

$$x=\delta; \frac{\partial C_{b,i}}{\partial x} = 0$$

Non-wetted biofilm

$$\frac{\partial C_{b-NW,i}}{\partial t} = D_{eff,i} \frac{\partial^2 C_{b-NW,i}}{\partial x^2} - r_{b-NW,i} - OUR_{end} \quad (6)$$

with boundary conditions:

$$t=0; C_{b-NW,i} = C_{b-NW,i}^0$$

$$x=0; C_{b-NW,i} = \frac{C_{g,i}}{He_i}$$

$$x=\delta; \frac{\partial C_{b-NW,i}}{\partial x} = 0$$

4

5 $C_{g,i}^{Bed}$, $C_{l,i}^{Bed}$, $C_{b,i}$ and $C_{b-NW,i}$ are the concentrations of component i in the bulk gas phase, bulk liquid

6 phase, biofilm and non-wetted biofilm, respectively (g m^{-3}); $C_{g,i}^{Free}$, $C_{l,i}^{Res}$ are the concentrations of

7 component i in the free gas volume and in the liquid reservoir tank respectively (g m^{-3}); He_i is

8 the gas/liquid partition coefficient of component i (dimensionless); a , a_{g-l} , a_{l-b} , a_{g-b} (see Eqs. 8-

9 10) represent the specific surface area per volume unit of packed bed, gas-liquid specific

10 contact area, liquid-biofilm specific contact area and gas-biofilm specific contact area,

11 respectively ($\text{m}^2 \text{m}^{-3}$); $D_{eff,i}$ is the diffusion coefficient of component i in the biofilm ($\text{m}^2 \text{h}^{-1}$);

1 $r_{b,i}$, $r_{b-NW,i}$ are the consumption rates of component i in the wetted biofilm and in the non-
 2 wetted biofilm respectively ($\text{g m}^{-3} \text{h}^{-1}$); δ is the biofilm thickness (m).

3

4 **2.5.4. Model solution**

5 N is the total number of layers of the discretized biofilm thickness for the numerical resolution
 6 of the mathematical model. According to Eq. (7), K_B is the external mass transfer coefficient
 7 from external bulk phase to biofilm. The surface fraction of the packing material covered by
 8 biofilm (β) was estimated according to Eq. (11).

9

$$10 \quad K_B = \frac{D_{eff,i} \cdot N}{\delta} \quad (7)$$

$$11 \quad a_{g-l} = a \cdot \alpha \quad (8)$$

$$12 \quad a_{l-b} = \beta \cdot a_{g-l} \quad (9)$$

$$13 \quad a_{g-b} = (a - a_{g-l}) \cdot \beta \quad (10)$$

$$14 \quad \beta = \frac{\epsilon_b^{bed}}{a \cdot \delta} \quad (11)$$

15

16 The set of partial differential equations was discretized in space along the biofilm thickness.
 17 Six points were used along the biofilm thickness. The resulting set of ordinary differential
 18 equations was solved using a Rosenbrock (stiff) integration method with Berkeley Madonna
 19 8.3.18.

20

21 **2.5.5. Microbial kinetics**

1 The OUR within the biofilm was described by a double Monod-Haldane type kinetic
 2 expression depending on dissolved oxygen and dissolved H₂S concentrations inside the biofilm
 3 (Eqs. 12 and 13). The H₂S uptake rate was computed from Eqs. (14) and (15) as a function of
 4 the stoichiometric yield of sulfide oxidation.

5

6 Wetted biofilm:

$$r_{b,O_2} = OUR_{\max} \left(\frac{C_{b,O_2}}{C_{b,O_2} + K_{S,O_2}} \right) \left(\frac{C_{b,H_2S}}{K_{S,H_2S} + C_{b,H_2S} + \frac{(C_{b,H_2S})^2}{k_I}} \right) \quad (12)$$

7 Non-wetted-biofilm:

$$r_{b-NW,O_2} = OUR_{\max} \left(\frac{C_{b-NW,O_2}}{C_{b-NW,O_2} + K_{S,O_2}} \right) \left(\frac{C_{b-NW,H_2S}}{K_{S,H_2S} + C_{b-NW,H_2S} + \frac{(C_{b-NW,H_2S})^2}{k_I}} \right) \quad (13)$$

8 While:

$$r_{b,H_2S} = \frac{r_{b,O_2}}{Y_{O_2/H_2S}} \quad (14)$$

$$r_{b-NW,H_2S} = \frac{r_{b-NW,O_2}}{Y_{O_2/H_2S}} \quad (15)$$

9

10 2.5.6. Stoichiometry of H₂S oxidation

11 Recent reports [15] stated that elemental sulfur or sulfate production occur depending on the
 12 molar ratio of dissolved oxygen and sulfide species in the biofilm, namely [O₂]/[H₂S] ratio. At
 13 molar ratios [O₂]/[H₂S] ≤ 1.0 H₂S oxidation occurs through Eq. (16) at a stoichiometric yield
 14 $Y_{O_2/H_2S} = 0.5$ while Eq. (17) predominates at a stoichiometric yield $Y_{O_2/H_2S} = 2.0$ when the molar
 15 ratio [O₂]/[H₂S] > 1.0. During modeling of respirometric assays, the molar ratio [O₂]/[H₂S] in

1 the biofilm was evaluated at each integration step of the differential equations set in order to
 2 predict the fate of H₂S oxidation. A step switch function was programmed to use the
 3 corresponding molar yield.

4



5

6 Furthermore, the calibrated model was used to predict the transient H₂S elimination capacity of
 7 the biotrickling filter bed (g H₂S m⁻³ bed h⁻¹) considering the fate of H₂S as well as the
 8 contribution of wetted and non-wetted biofilm to H₂S elimination according to Eq. (18).

9

$$EC_{\text{H}_2\text{S}} = \left[(r_{b,\text{O}_2} \cdot a_{l-b}) + (r_{b-\text{NW},\text{O}_2} \cdot a_{g-b}) \right] \cdot \frac{\delta}{0.94 \cdot Y_{\text{O}_2/\text{H}_2\text{S}}} \quad (18)$$

10

11 Where 0.94 corresponds to a conversion factor from molar to mass units (mol O₂ mol⁻¹ H₂S to g
 12 O₂ g⁻¹ H₂S).

13

14 2.6. Model parameters estimation

15 Physical and some biokinetic parameters included in the model were either experimentally
 16 determined or taken from literature while others were obtained from the packing materials
 17 manufacturers (Table 1).

18

Here Table 1.

1
2
3
4
5
6
7
8
9
10
11
12
13

The experimental gaseous and dissolved oxygen concentration profiles generated from the respective respirometric tests were used to calibrate the mathematical model described above. Only three biokinetic (OUR_{max} , K_{S,H_2S} and K_{i,H_2S}) and one morphological parameters (biofilm thickness δ) were determined by fitting the experimental data. Parameters estimation was performed following the least square method by minimizing the quadratic error between model predictions and measured gaseous and dissolved oxygen concentrations. Model simulations and parameters estimation were performed with Berkeley Madonna 8.3.18 software. A statistical analysis based on paired t-student tests at a 5% level of significance were performed for dissolved oxygen and oxygen gas in both packing materials in order to quantify the agreement between results predicted by the model with the optimized kinetic parameters and experimental data.

14 **3. RESULTS**

15 **3.1. Abiotic tests**

16 Fig. 3 shows the $K_L a_{g-l}$ as a function of the hydrodynamic conditions for both packing materials. Results indicated that the gas velocity had a larger impact on $K_L a_{g-l}$ compared to the impact of increasing the liquid velocity for both packing materials. Here the unexpected effect of the increase of gas velocity on the $K_L a_{g-l}$ can be due to the excessive mixing of liquid, which caused a sensible reduction of the resistance to the mass transport in the liquid side. Also, slightly higher mass transfer coefficients were found for PR compared to PUF under all conditions tested. Hydrodynamic conditions that lead to a $K_L a_{g-l}$ of around 20 h^{-1} (gas and

1 liquid flow rates of 43.4 m h^{-1} and 10.8 m h^{-1} , respectively) were selected as convenient for
2 biofiltration operation according to Kim and Deshusses [5]. Therefore, such conditions were set
3 for subsequent biotic tests.

4 *Here Figure 3.*

5 **3.2. Model calibration in biotic tests**

6 Fig. 4 shows the oxygen concentration changes in gas and liquid phases induced due to the
7 biological H_2S oxidation in the corresponding packed bed tested. The total biofilm mass
8 experimentally assessed on PR and PUF was 2.1 and 7.0 g VSS, respectively. Solid lines show
9 the HR model predictions after optimization of OUR_{max} , δ , K_{s,H_2S} and K_{i,H_2S} for both packing
10 materials. Overall, a good agreement was found for the oxygen profiles in the gas phase for
11 both packing materials. Also, the dissolved oxygen concentration predicted for the PR packing
12 was satisfactory (Fig.4A) while a slight overestimation of the oxygen consumption was found
13 for PUF towards the end of the test. The t-Student tests executed for all variables in Fig. 4 (C_{l,O_2}
14 and C_{g,O_2}) yielded absolute values in between the two t-test tails at a 5% level of significance
15 indicating that the differences between dissolved oxygen and oxygen gas measured
16 experimentally and those predicted by the model were not statistically significant in the studied
17 period for PUF.

18

Here Figure 4.

1 The fitted parameters as well as other relevant estimates calculated from model estimates are
2 shown in Table 2. At the trickling rate tested (10.8 m h^{-1}), the fraction of biofilm covered by
3 water (assuming to be proportional to α) was much smaller than that directly exposed to the gas
4 for both packing materials. Even if the thickness of the biofilm on PUF was more than half that
5 of the PR, the surface of packing covered by biofilm (β), the area of biofilm directly exposed to
6 the gas phase (a_{g-b}) as well as the OUR_{max} were significantly larger for the PUF packing
7 compared to those for the PR. Results in Table 2 indicate that a combination of several factors
8 lead to find a larger H_2S elimination capacity for the PUF packing. The external oxygen mass
9 transfer coefficients K_L and K_B would explain such differences as discussed later.

Here Table 2.

10

11 Similarly, the overall capacity for H_2S degradation must consider not only mass transport but
12 also the biological activity inside the biofilm. Table 2 also shows the maximum EC estimated
13 by the model corresponding to the maximum activity along the biotic test for each packing
14 material (Fig. 5). The experimental EC during the whole respirometric assay for both type
15 kinetic assays was around $52 \text{ g H}_2\text{S m}^{-3} \text{ h}^{-1}$ which was much lower than the maximum EC
16 predicted by the model. Such a difference can be explained by the fact that the maximum EC is
17 computed at a specific time under favorable oxygen and H_2S concentrations in the biofilm,
18 while on the other the conditions during the respective respirometric assay changed from

1 nearby inhibitory to limiting H_2S concentrations, this resulted in an averaged EC value that
2 underestimates the potential EC of the colonized sampled bed

3 Oppositely to that of PR, the EC estimated for PUF indicated that H_2S was almost depleted at
4 the end of the test. In the first 2 minutes an initial lag phase was found for both packing
5 materials. As commonly found in respirometric tests performed in SCR, such behavior was
6 related to the wake-up time needed by microorganisms for adapting to the test conditions after
7 the endogenous phase. Also, model predictions based on the contribution of the wetted and
8 non-wetted fraction as calculated by Eq. (18) indicated that the non-wetted biofilm fraction in
9 both packing materials contributed in average around 65% to the EC observed (Fig. 5).

Here Figure 5.

10

11 **3.3. Assessment of the rate controlling step**

12 Although no experimental data of the concentrations of the species inside the biofilm was
13 available at the time of the study, the calibrated HR model was used to predict the theoretical
14 profiles of the electron donor and acceptor inside the biofilm at two particular times of the
15 respirometry. First, at the time of reaching the maximum H_2S elimination capacity EC_{max} ,
16 namely t_{max} , and secondly at the end of the test, namely t_{end} (Fig. 5). Fig. 6 shows the predicted
17 concentrations of H_2S and dissolved oxygen inside of the wetted and non- wetted biofilm for
18 both packing materials at both t_{max} and t_{end} . In Fig. 6A and 6B for the wetted biofilm a similar
19 behavior can be observed for both colonized packed beds independently of the time at which
20 profiles were assessed. Almost the whole biofilm was active in both cases except in the inner

1 layers of the PUF biofilm at t_{end} (Fig. 6B) since H_2S had been almost completely consumed at
2 the end of the test. Except in the latter case, no substrate limitation occurred in the wetted
3 fractions of the biofilm. For PUF at t_{max} (Fig. 6D), the H_2S elimination capacity in the non-
4 wetted biofilm was limited by the diffusion of oxygen through the biofilm. The inner layers
5 turned out to be inactive for both packing materials.

6 *Here Figure 6.*

7 Since different H_2S and O_2 concentrations in the biofilm existed along time and biofilm depth,
8 the H_2S elimination rates and its controlling factor depended on the molar $[\text{O}_2]/[\text{H}_2\text{S}]$ ratio
9 which, in turn, defined the products of H_2S oxidation. Fig. 7 shows the molar $[\text{O}_2]/[\text{H}_2\text{S}]$ ratio
10 through the biofilm thickness computed at the same time than those in Fig. 6. According to
11 Eqs. (14) and (15), a combination of elemental sulfur and sulfate were being produced in both
12 packing materials.

13 *Here Figure 7.*

14 **4. DISCUSSION**

15 The use of bacterial biofilm as catalyst for the desulfurization of biogas in biotrickling filters is
16 highly convenient in terms of its easy design and operation, but difficult to keep good
17 performance if not enough knowledge about the complex phenomena occurring in the
18 biofiltration process is available. Oppositely to SCR, HR can mimic the hydrodynamic

1 conditions found in a BTF allowing the estimation of the intrinsic biological activity of the
2 biofilm by inducing comparative boundary layer properties of the mobile phases. Besides, the
3 HR methodology described in this work considers and quantifies phenomena such as the partial
4 wetting of both the packing and biofilm that occur in real biotrickling filters.

5 Abiotic tests performed for the packing materials under study indicated that both packing
6 materials showed similar performance and values for the oxygen $K_L a_{g-l}$. Kim and Deshusses
7 [21] suggested a proportional relationship of the liquid linear velocities to the $K_L a$ of oxygen,
8 which was confirmed in this work. Despite of the lower specific surface area of PR compared
9 to PUF, slightly higher $K_L a_{g-l}$ values for PR were found. Characterization of PUF in several
10 works has shown that the reticulate structure of PUF provides a large accumulation of water in
11 packed beds in the form of water droplets [22]. Both results suggest that such water
12 accumulation in PUF does not necessarily improve G-L mass transfer if water is not well
13 distributed as a thin layer over the surface of the packing material. In fact, Table 2 shows that α ,
14 the fraction of the packing surface covered with water, was estimated to be similar for PR and
15 PUF [5]. Then, the larger bulk porosity of PUF does not correspond to a better water trickling
16 since a fraction of the water accumulated inside the foam may not be accessible for G-L mass
17 transfer. Therefore, water and biofilm distribution over the surface of both packing materials
18 had a large impact in the performance of the system as shown in biotic tests.

19 In biotic assays, t-Student test showed that model predictions were in good agreement with
20 experimental results indicating that mass transport and biological kinetics were satisfactorily
21 included in the HR model. Biofilm concentration profiles presented in Fig. 6 indicated that the
22 wetted biofilm had a limited G-L oxygen transport compared to that of H_2S , i.e. solubility,
23 which could have conditioned the bioreaction rate at first layers of biofilm, due to slightly

1 larger accumulation of H_2S at t_{max} in the wetted biofilm than the accounted for the non-wetted
2 biofilm. According to González-Sánchez et al. [23], at concentrations >15 mM H_2S a partial
3 substrate inhibition of the H_2S degradation rate could occur, explaining why almost all wetted
4 biofilm was active but not fast enough. The H_2S external transport was not relevant here
5 because of its much higher solubility ($He=0.41$) compared to that of oxygen ($He=32$) under
6 standard conditions. In the non-wetted biofilm, where no external mass transport resistance
7 existed, bioreaction rates were maximized in the external layers but minimized in the deeper
8 layers of the biofilm. This observation previously find by others [24-25] indicates that both
9 oxygen and H_2S diffusion rates through biofilm limited the activity of the biofilm.

10 Results also allowed calculating the contribution of the wetted and non-wetted fractions to the
11 total flux of H_2S and O_2 to the biofilm. Since wetted surfaces ($a_{l,b}$) were lower for PR and PUF
12 compared to the non-wetted surface (a_{g-b}), the contribution of the G-L flux and that of the G-B
13 flux was significantly different for both packing materials. According to the mass transport
14 terms in Eq. (1), the oxygen G-B flux was 0.53 g O_2 m^{-2} h^{-1} , while the corresponding G-L flux
15 was 0.23 g O_2 m^{-2} h^{-1} for PUF. Similarly, gas fluxes of 0.41 and 0.05 g O_2 m^{-2} h^{-1} for G-B and
16 G-L fluxes, respectively, were found for PR. Nevertheless, the H_2S elimination capacity
17 predicted by the model (Eq. (18)), scrutinized in average that around 65% of the H_2S
18 eliminated in the BTF was due to the non-wetted biofilm for both packing materials tested,
19 similar trend was reported by Li et al. [26]. However, a different behavior to the oxygen fluxes
20 was computed for H_2S , resulting in a G-L flux slightly higher than the G-B flux, which can be
21 explained in terms of the gradient concentrations conditioning the mass fluxes (Eq. (1)). In the
22 case of H_2S , these concentration gradients were similar either for G-L and G-B interphases,
23 which indicated that no external mass transfer limitation of H_2S occurred, mainly due to its

1 much higher solubility than that of oxygen. Here the H₂S solubility can be sensibly enhanced
2 by its absorption in aqueous solutions at pH>7 [27]. In addition, experimental results about
3 biomass density indicated that the biofilm amount on the PUF was twice larger than that on PR,
4 so different distribution in the bed leads to key consequences in terms of H₂S removal. In the
5 case of PUF, a thinner biofilm, as well as a larger surface colonized by biofilm than that
6 obtained with PR lead to a PUF biofilm much more active (4 times compared with PR taking as
7 reference the EC_{max}) with a larger capacity for oxygen consumption and concomitant H₂S
8 degradation. Overall, results are consistent with the common experimental evidence that a
9 higher water hold-up in biotrickling filters leads to reduced EC and removal efficiencies [21,
10 28-30] and especially for poorly soluble compounds as O₂. In any case, results presented herein
11 become in an interesting theoretical framework in the sense that previous models that
12 considered wetted and non-wetted biofilms either took into account only the absorption of
13 pollutant in the G-L interphase [24-25] or did not analyze the contribution G-L and G-B mass
14 fluxes [5]. Results herein point out that both G-B as well as G-L transfer fluxes must be
15 considered and analyzed separately depending on the solubility of each compound.

16 The model predicted that maximum EC for H₂S occurred close to or under oxygen limiting
17 conditions in both wetted and non-wetted biofilms. Reported H₂S elimination capacities are
18 between 50 to 400 g H₂S m⁻³ h⁻¹ [5, 14, 31-32] for different BTFs packed with various
19 materials and operated under similar conditions, which were in general lower than the predicted
20 by the calibrated mathematical model. This fact shows that conventional BTFs could not be
21 optimally operated, meaning that the biofilm has to be exposed to optimal H₂S concentrations
22 (non-limiting and non-inhibiting) as well as non-limiting oxygen concentrations. These ideal
23 conditions could be very difficult to reach, especially in full-scale BTFs, where probably a

1 large percentage of biofilm has low or no H₂S-oxidizing activity. As pointed out by other
2 authors, the use of intensive devices for O₂ transport to the liquid phase, which is the main
3 bottleneck when high loads of H₂S are removed, may help to improve the performance of BTFs
4 [33].

5 Also, model predictions helped understanding the different instant by-products production from
6 H₂S biological oxidation in a range of situations. Although at the end of the tests an oxygen
7 excess condition was reached and, concomitantly, sulfate was the main product of H₂S
8 oxidation (Fig. 7), elemental sulfur was the main product in almost all situations for PR.
9 Elemental sulfur could be only produced in the inner layers of the non-wetted biofilm at t_{max} for
10 PUF. The molar ratios [O₂]/[H₂S] predicted inside of the biofilm indicate that maximum
11 elimination capacities should be reached under oxygen limiting conditions in the first layers,
12 but this means to overload the biofilm with H₂S. This could induce several performance risks,
13 i.e. reaching inhibitory H₂S concentrations (>0.15 mM) [23] or clogging the biofilter bed by
14 excessive formation and accumulation of elemental sulfur [34-36]. Instead, excess oxygen is
15 desirable in terms of biofilter operation, but expensive because of the need to keep neutral pH
16 (see Eq. (14)) as well as to promote adequate oxygen transfer if high loading rates of H₂S are
17 treated [4]. Other factors not considered herein such as the reticulate structure of PUF must be
18 also included in order to analyze the performance of different packing materials based on the
19 HR. As an example, the larger biomass retention capacity of PUF may be counterproductive
20 when elemental sulfur is produced in the bed.

21 Overall, experimental data of the gas and the liquid phases to both describe mass transfer and
22 biological activity showed that dissolved oxygen and O₂ profiles allowed to assess the
23 biological activity of a sample of packing material from a packed bed biological reactor and to

1 provide a theoretical benchmark to explain such behavior. It is worth mentioning that model
2 predictions in terms of the concentrations of the species in the biofilm phase as well as several
3 model parameters are influenced by the lack of experimental data from inside the biofilm
4 phase. Data other than oxygen, which may include the fate of sulfide and its degradation
5 subproducts, is warranted for improving the modeling approach proposed herein, even if data in
6 such type of systems is difficult, even impossible in some cases, to obtain. Most modeling
7 literature, dealing with biofilters and biotrickling filters, report only gas phase data [37-40]
8 while almost no literature reports data inside biofilms since complex setups are needed and
9 only few probes available. As an example, sulfur production or deposition, which would serve
10 to better understand the H₂S oxidation cannot be measured directly. Elemental sulfur
11 measurements are not reliable, even less in complex biofilm growth as that occurring in PUR
12 supports [41]. The common practice is to calculate elemental sulfur production based on mass
13 balances between the sulfide removed and the sulfate produced [32, 42-43] , which cannot be
14 measured either. Developing monitoring tools and methods for obtaining additional data from
15 biofilms is warranted for improving our modeling approach and to gain knowledge and
16 robustness in the models proposed [44]. Such data together with a classical sensitivity analysis
17 [45] would also contribute to reduce uncertainty of model parameters estimation. In fact, no
18 work in literature has attempted to analyze neither the structural nor the parameter
19 identifiabilities [46] of biofiltration models. It is well-known that modeling of biofiltration
20 systems is based on models with a large number of parameters and processes that may be
21 correlated which, coupled to a common lack of data of the biofilm (biofilm composition and
22 structure, concentration of species in the biofilm...), lead to solutions that are fairly recognized
23 as non-unique. However, the lack of such analysis/data and parameter correlation do not
24 invalidate modeling efforts.

1 **5. CONCLUSIONS**

2 In this study heterogeneous respirometry was successfully applied to characterize the basic
 3 biofiltration properties (i.e. transport and biological phenomena) using a small and
 4 representative piece of packing material from an operating biotrickling filter in a short period of
 5 time, which allowed considering the biofilm properties as constant. Evaluation of mass
 6 transport by mimicking the hydraulic conditions of a BTF during the respirometric assays
 7 allowed estimating the contribution of wetted and non-wetted biofilms fractions to the overall
 8 removal of H₂S as well as to determine the limiting step. Then intrinsic biokinetic parameters
 9 were estimated with the minimal handling of the biofilm. This technique has shown to be
 10 highly adequate to study the kinetics of immobilized biomass which is essential in those
 11 generic models describing biofiltration process or other similar process involving biofilms.
 12 However, more data is needed, particularly from substrate degradation and inside the biofilm,
 13 to reduce uncertainty of model parameters estimation as well as to verify model predictions.

14 **LIST OF SYMBOLS**

15 a_{g-b} = gas-biofilm specific surface area, m² m⁻³

16 a_{g-l} = gas-liquid specific surface area, m² m⁻³

17 a_{l-b} = liquid-biofilm specific surface area, m² m⁻³

18 $C_{g,i}^{Bed}$ = concentration of component i in the gas phase in the bed, g m⁻³

19 $C_{g,i}^{Free}$ = concentration of component i in the gas phase in the free section, g m⁻³

20 $C_{l,i}^{Bed}$ = concentrations of component i in the liquid phase in the bed, g m⁻³

- 1 $C_{l,i}^{\text{Res}}$ = concentrations of component i in the liquid phase in the reservoir section, g m^{-3}
- 2 $D_{\text{eff},i}$ = diffusion coefficient of component i in the biofilm, $\text{m}^2 \text{h}^{-1}$
- 3 EC = elimination capacity, $\text{g m}^{-3} \text{h}^{-1}$
- 4 He_i = gas/liquid partition coefficient of component i in a air/aqueous system
- 5 K_B = the external mass transfer coefficient from external bulk phase to biofilm, m h^{-1}
- 6 $K_{La_{g-l}}$ = global mass transfer coefficient, h^{-1}
- 7 k_i = saturation constant for component i , g m^{-3}
- 8 $K_{s,i}$ = half saturation constant for component i , g m^{-3}
- 9 N = total number of layers that thickness biofilm was divided for the numerical resolution of
- 10 the mathematical model
- 11 OUR = oxygen uptake rate, $\text{g O}_2 \text{m}^{-3} \text{h}^{-1}$
- 12 OUR_{max} = maximum oxygen uptake rate, $\text{g O}_2 \text{m}^{-3} \text{h}^{-1}$
- 13 OUR_{end} = endogenous oxygen uptake rate, $\text{g O}_2 \text{m}^{-3} \text{h}^{-1}$
- 14 Q_g = gaseous volumetric flow rate, $\text{m}^3 \text{h}^{-1}$
- 15 Q_l = liquid volumetric flow rate, $\text{m}^3 \text{h}^{-1}$
- 16 $r_{b,i}$ = consumption rates of component i in the wetted biofilm, $\text{g m}^{-3} \text{h}^{-1}$
- 17 $r_{b-NW,i}$ = consumption rates of component i in the non-wetted biofilm, $\text{g m}^{-3} \text{h}^{-1}$
- 18 t = time, h

1 t_{end} = final time of respirometry assay, h

2 t_{max} = time when maximum elimination capacity occurred, h

3 V_{bed} = packed bed volume, m³

4 V_{bio} = biomass volume, m³

5 V_g = gaseous volume, m³

6 V_l = liquid volume, m³

7 x = thickness position in the biofilm, m

8 Y_{O_2/H_2S} = yield coefficient, mol O₂ mol⁻¹ H₂S

9

10 Subscripts

11 b = section of biofilm wetted

12 $b-NW$ = section of biofilm non-wetted

13 i = component i

14 max = maximum

15

16 Superscripts

17 Bed = packed bed of HR

18 $Free$ = gas free volume

19 Res = reservoir liquid volume

1

2 Greek Letters3 α = surface fraction of packing material wetted4 β = surface fraction of the packing material covered by biofilm5 δ = biofilm thickness, m6 ε_l^{Bed} = volume fraction occupied by the liquid in the packed bed, $\text{m}^3 \text{m}^{-3}$ 7 ε_g^{Bed} = volume fraction occupied by the gas in the packed bed, $\text{m}^3 \text{m}^{-3}$ 8 ε_b^{Bed} = volume fraction occupied by the biofilm in the packed bed, $\text{m}^3 \text{m}^{-3}$

9

10 **Acknowledgements**

11 The Spanish government (MEC) provided financial support through the project CTM2009-
12 14338-C03-01 and CTM2012-37927-C03-01. The Department of Chemical Engineering at
13 UAB (Universitat Autònoma de Barcelona) is a unit of Biochemical Engineering of the Xarxa
14 de Referència en Biotecnologia de Catalunya (XRB), Generalitat de Catalunya. The financial
15 support of National Council of Science and Technology of Mexico CONACyT (CB-
16 2011/168288) is also gratefully acknowledged.

17

1 **REFERENCES**

- 2 [1] N. Abatzoglou, S. Boivin, A review of biogas purification processes, *Biofuels Bioprod.*
3 *Biorefining*, 3 (2009) 42-71.
- 4 [2] E. Ryckebosch, M. Drouillon, H. Veruaeren, Techniques for transformation of biogas to
5 biomethane, *Biomass Bioenerg.*, 35 (2011) 1633-1645.
- 6 [3] H.H.J. Cox, M.A. Deshusses, Biological waste air treatment in biotrickling filters, *Curr.*
7 *Opin. Biotechnol.*, 9 (1998) 256-262.
- 8 [4] M. Fortuny, J.A. Baeza, X. Gamisans, C. Casas, J. Lafuente, M.A. Deshusses, D. Gabriel,
9 Biological sweetening of energy gases mimics in biotrickling filters, *Chemosphere*, 71
10 (2008) 10-17.
- 11 [5] S. Kim, M.A. Deshusses, Development and experimental validation of a conceptual model
12 for biotrickling filtration of H₂S, *Environ. Prog.*, 22 (2003) 119-128.
- 13 [6] H. Spanjers, P. Vanrolleghem, *Respirometry as a tool for rapid characterization of*
14 wastewater and activated sludge, *Water Sci. Technol.*, 31 (1995) 105-114.
- 15 [7] P.A. Vanrolleghem, H. Spanjers, B. Petersen, P. Ginestet, I. Takacs, Estimating
16 (combinations of) Activated Sludge Model No. 1 parameters and components by
17 respirometry, *Water Sci. Technol.*, 39 (1999) 195-214.
- 18 [8] A.K. Gernaey, B. Petersen, J.P. Ottoy, P. Vanrolleghem, Activated sludge monitoring with
19 combined respirometric-titrimetric measurements, *Water Res.*, 35 (2001) 1280-1294.
- 20 [9] A. Guisasola, M. Pijuan, J.A. Baeza, J. Carrera, C. Casas, J. Lafuente, Aerobic phosphorus
21 release linked to acetate uptake in bio-P sludge: Process modeling using oxygen uptake
22 rate, *Biotechnol. Bioeng.*, 85 (2004) 722-733.
- 23 [10] I. Garcia-Pena, S. Hernandez, R. Auria, S. Revah, Correlation of biological activity and
24 reactor performance in biofiltration of toluene with the fungus *Paecilomyces variotii*
25 CBS115145, *Appl. Environ. Microbiol.*, 71 (2005) 4280-4285.
- 26 [11] R. Govind, W. Zhao, D.F. Bishop, Biofiltration kinetics for volatile organic compounds
27 (VOCs) and development of a structure-biodegradability relationship, in: 90th Annual
28 Meeting and Exhibition of the Air and Waste Management Association, Pittsburg, PA,
29 USA, 1997.
- 30 [12] R. Ramirez-Vargas, A. Ordaz, M. Carrion, I.Y. Hernandez-Paniagua, F. Thalasso,
31 Comparison of static and dynamic respirometry for the determination of stoichiometric and
32 kinetic parameters of a nitrifying process, *Biodegradation*, 24 (2013) 675-684.
- 33 [13] M. Piculell, T. Welander, K. Jonsson, Organic removal activity in biofilm and suspended
34 biomass fractions of MBBR systems, *Water Sci. Technol.*, 69 (2014) 55-61.
- 35 [14] A.M. Montebello, M. Fernandez, F. Almenglo, M. Ramirez, D. Cantero, M. Baeza, D.
36 Gabriel, Simultaneous methylmercaptan and hydrogen sulfide removal in the
37 desulfurization of biogas in aerobic and anoxic biotrickling filters, *Chem. Eng. J.*, 200
38 (2012) 237-246.

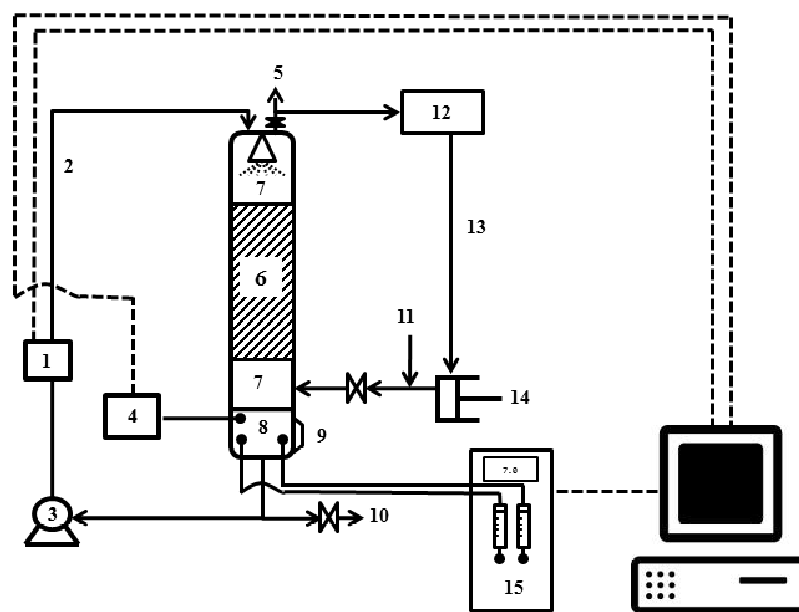
- 1 [15] J.B.M. Klok, P.L.F. van den Bosch, C.J.N. Buisman, A.J.M. Stams, K.J. Keesman, A.J.H.
2 Janssen, Pathways of sulfide oxidation by haloalkaliphilic bacteria in limited-oxygen gas
3 lift bioreactors, *Environ. Sci. Technol.*, 46 (2012) 7581-7586.
- 4 [16] D. Green, R. Perry, *Perry's Chemical Engineers' Handbook*, Mc. Graw-Hill, New York,
5 2007.
- 6 [17] V. Lazarova, J. Manem, Biofilm characterization and activity analysis in water and
7 wastewater treatment, *Water Res.*, 29 (1995) 2227-2245.
- 8 [18] W.C. Hugler, J. Cantu-De la Garza, M. Villa-Garcia, Biofilm analysis from an odor-
9 removing trickling filter, in: 89th Annual Meeting and Exhibition of the Air and Waste
10 Management Association, Pittsburg, PA, USA, 1996.
- 11 [19] A. Gonzalez-Sanchez, L. Arellano-Garcia, W. Bonilla-Blancas, G. Baquerizo, S.
12 Hernandez, D. Gabriel, S. Revah, Kinetic characterization by respirometry of VOC-
13 degrading biofilms from gas-phase biological filters, *Ind. Eng. Chem. Res.*, (2014)
14 Accepted.
- 15 [20] A. Gonzalez-Sanchez, G. Baquerizo, X. Gamisans, J. Lafuente, D. Gabriel, Short term
16 characterization of a H₂S biotrickling filter packing using a gaseous-liquid respirometer, in:
17 3rd International Congress on Biotechniques for Air Pollution 2009, pp. 255-260.
- 18 [21] S. Kim, M.A. Deshusses, Determination of mass transfer coefficients for packing materials
19 used in biofilters and biotrickling filters for air pollution control - 2: Development of mass
20 transfer coefficients correlations, *Chem. Eng. Sci.*, 63 (2008) 856-861.
- 21 [22] A.D. Dorado, F.J. Lafuente, D. Gabriel, X. Gamisans, A comparative study based on
22 physical characteristics of suitable packing materials in biofiltration, *Environ. Technol.*, 31
23 (2010) 193-204.
- 24 [23] A. Gonzalez-Sanchez, M. Tomas, A.D. Dorado, X. Gamisans, A. Guisasola, J. Lafuente,
25 D. Gabriel, Development of a kinetic model for elemental sulfur and sulfate formation
26 from the autotrophic sulfide oxidation using respirometric techniques, *Water Sci. Technol.*,
27 59 (2009) 1323-1329.
- 28 [24] C.J. Mpanias, B.C. Baltzis, An experimental and modeling study on the removal of mono-
29 chlorobenzene vapor in biotrickling filters, *Biotechnol. Bioeng.*, 59 (1998) 328-343.
- 30 [25] B.C. Baltzis, C.J. Mpanias, S. Bhattacharya, Modeling the removal of VOC mixtures in
31 biotrickling filters, *Biotechnol. Bioeng.*, 72 (2001) 389-401.
- 32 [26] H. Li, J.C. Crittenden, J.R. Mihelcic, H. Hautakangas, Optimization of biofiltration for
33 odor control: model development and parameter sensitivity, *Water Environ. Res.*,
34 (2002) 5-16.
- 35 [27] A. Gonzalez-Sanchez, S. Revah, The effect of chemical oxidation on the biological sulfide
36 oxidation by an alkaliphilic sulfoxidizing bacterial consortium, *Enzyme Microbiol.*
37 *Technol.*, 40 (2007) 292-298.
- 38 [28] S. Kim, M.A. Deshusses, Understanding the limits of H₂S degrading biotrickling filters
39 using a differential biotrickling filter, *Chem. Eng. J.*, 113 (2005) 119-126.

- 1 [29] S. Kim, M.A. Deshusses, Determination of mass transfer coefficients for packing materials
2 used in biofilters and biotrickling filters for air pollution control. 1. Experimental results,
3 Chem. Eng. Sci., 63 (2008) 841-855.
- 4 [30] N. Abdehagh, M.T. Namini, B. Bonakdarpour, S.M. Heydarian, Effect of operating
5 parameters on the performance of a *Thiobacillus thioparus*-immobilized polyurethane
6 foam biotrickling filter for hydrogen sulfide removal, Clean-Soil Air Water, 42 (2014)
7 1311-1317.
- 8 [31] A. Tamimi, E.B. Rinker, O.C. Sandall, Diffusion coefficients for hydrogen sulfide, carbon
9 dioxide, and nitrous oxide in water over the temperature range 293-368-K, J. Chem. Eng.
10 Data, 39 (1994) 330-332.
- 11 [32] M. Ramirez, J.M. Gomez, G. Aroca, D. Cantero, Removal of hydrogen sulfide by
12 immobilized *Thiobacillus thioparus* in a biotrickling filter packed with polyurethane foam,
13 Biores. Technol., 100 (2009) 4989-4995.
- 14 [33] G. Rodriguez, A.D. Dorado, A. Bonsfills, R. Sanahuja, D. Gabriel, X. Gamisans,
15 Optimization of oxygen transfer through venturi-based systems applied to the biological
16 sweetening of biogas, J. Chem. Technol. Biotechnol., 87 (2012) 854-860.
- 17 [34] A.M. Montebello, M. Mora, L.R. López, T. Bezerra, X. Gamisans, J. Lafuente, M. Baeza,
18 D. Gabriel, Aerobic desulfurization of biogas by acidic biotrickling filtration in a randomly
19 packed reactor, J. Hazard. Mater., 280 (2014) 200-208.
- 20 [35] M. Tomàs, M. Fortuny, C. Lao, D. Gabriel, J. Lafuente, X. Gamisans, Technical and
21 economical study of a full-scale biotrickling filter for H₂S removal from biogas, Water
22 Pract. Technol., 4 (2009).
- 23 [36] M. Fortuny, A. Guisasola, C. Casas, X. Gamisans, J. Lafuente, D. Gabriel, Oxidation of
24 biologically produced elemental sulfur under neutrophilic conditions, J. Chem. Technol.
25 Biotechnol., 85 (2010) 378-386.
- 26 [37] G. Trejo-Aguilar, S. Revah, R. Lobo-Oehmichen, Hydrodynamic characterization of a
27 trickle bed air biofilter, Chem. Eng. J., 113 (2005) 145-152.
- 28 [38] J. Silva, M. Morales, M. Caceres, P. Morales, G. Aroca, Modelling of the biofiltration of
29 reduced sulphur compounds through biotrickling filters connected in series: Effect of H₂S,
30 Electron. J. Biotechnol., 15 (2012).
- 31 [39] A.K. Dhussa, S.S. Sambhi, S. Kumar, S. Kumar, J.K. Prajapati, Simplified simulation
32 model of a biotrickling filter used for the removal of hydrogen sulfide from biogas, Int. J.
33 Chem. React. Eng., 10 (2012).
- 34 [40] R. Lebrero, J.M. Estrada, R. Munoz, G. Quijano, Toluene mass transfer characterization in
35 a biotrickling filter, Biochem. Eng. J., 60 (2012) 44-49.
- 36 [41] L. Arellano-García, A. D.Dorado, A. Morales-Guadarrama, , E. Sacristan, X. Gamisans, S.
37 Revah, Modeling the effects of biomass accumulation on the performance of a biotrickling
38 filter packed with PUF support for the alkaline biotreatment of dimethyl disulfide vapors in
39 air. Appl. Microbiol. Biotechnol., 99 (2015) 97-107.

- 1 [42] R.B. Solcia, M. Ramirez, M. Fernandez, D. Cantero, D. Bevilaqua, Hydrogen sulphide
2 removal from air by biotrickling filter using open-pore polyurethane foam as a carrier,
3 *Biochem. Eng. J.*, 84 (2014) 1-8.
- 4 [43] Y.M. Jin, M.C. Veiga, C. Kennes, Effects of pH, CO₂, and flow pattern on the autotrophic
5 degradation of hydrogen sulfide in a biotrickling filter, *Biotechnol. Bioeng.*, 92 (2005)
6 462-471.
- 7 [44] X. Guimerà, A. Moya, A. Dorado, R. Villa, D. Gabriel, G. Gabriel, X. Gamisans, Biofilm
8 dynamics characterization using a novel DO-MEA sensor: mass transport and biokinetics,
9 *Appl. Microbiol. Biotechnol.*, (2014) 1-12.
- 10 [45] G. Baquerizo, J.P. Maestre, T. Sakuma, M.A. Deshusses, X. Gamisans, D. Gabriel, J.
11 Lafuente, A detailed-model of a biofilter for ammonia removal: Model parameters analysis
12 and model validation, *Chem. Eng. J.*, 113 (2005) 205-214.
- 13 [46] B. Petersen, K. Gernaey, M. Devisscher, D. Dochain, P.A. Vanrolleghem, A simplified
14 method to assess structurally identifiable parameters in Monod-based activated sludge
15 models, *Water Res.*, 37 (2003) 2893-2904.
- 16
17
18

1 **FIGURE CAPTIONS**

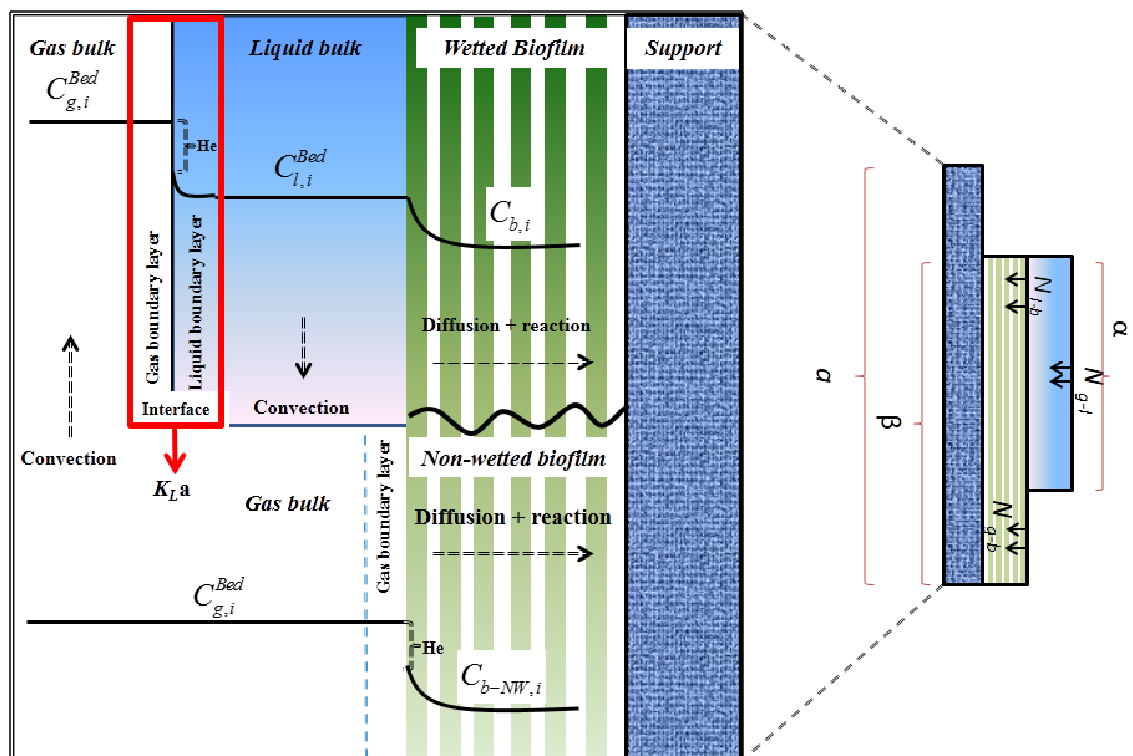
2



3

4 **Fig. 1.** Schematic of the Heterogeneous Respirometer. (1) dissolved oxygen sensor, (2) liquid
 5 recirculation, (3) Liquid recirculation pump, (4) pH sensor, (5) Gas out, (6) Packed bed, (7) Gas
 6 free (gas volume out of the packed bed), (8) Liquid reservoir, (9) Pulse port, (10) Liquid purge,
 7 (11) Gas in, (12) O₂/CO₂ sensor , (13) Gas recirculation, (14) Gas recirculation compressor,
 8 (15) micro-burette for pH control.

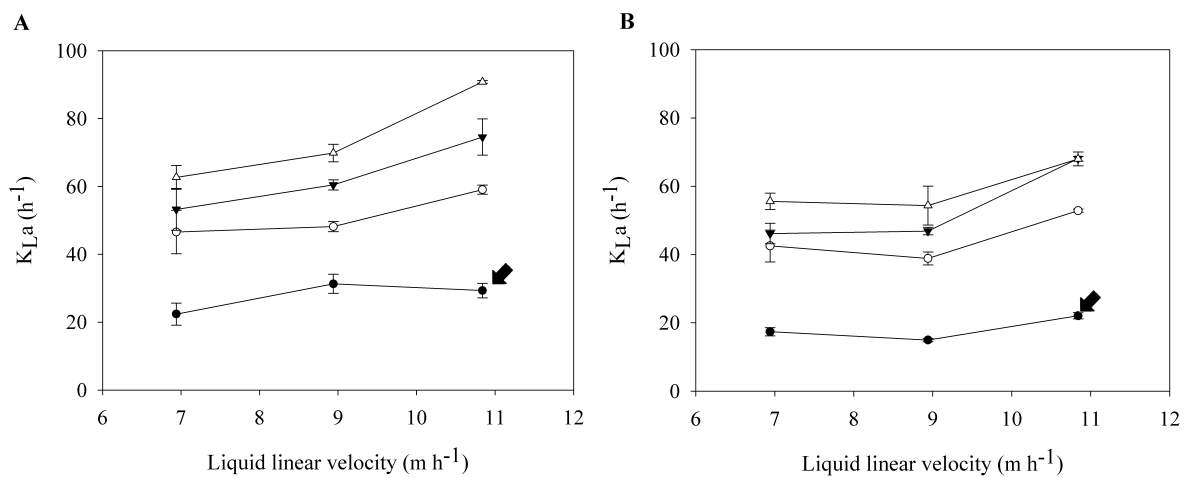
9



1

2 **Fig. 2.** Schematic of the phenomena and mechanisms of the H₂S removal in a biotrickling filter,3 assuming wetted and non-wetted biofilm. N_{l-b} , N_{g-l} , N_{g-b} refer to mass fluxes between phases.

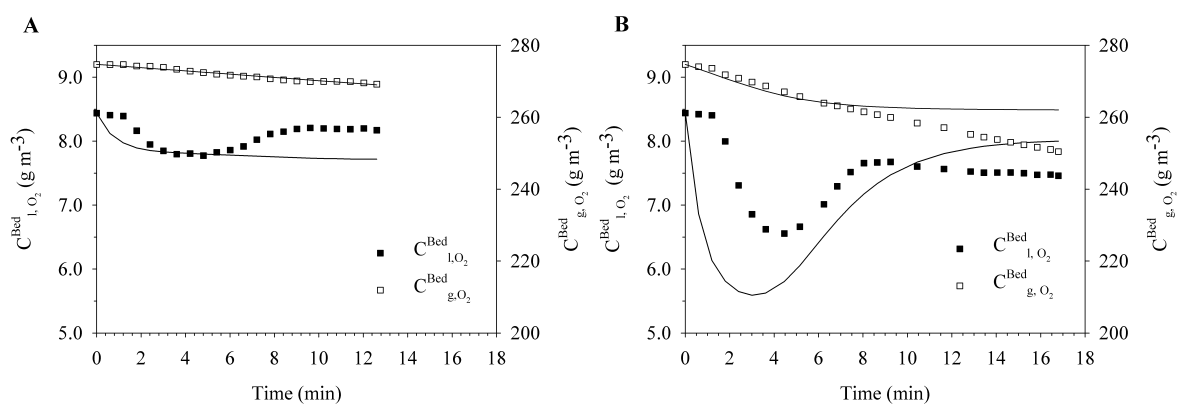
4



1

2 **Fig. 3.** Mass transfer coefficient for the two different packing materials tested at different gas
 3 and liquid flow rates. A) Stainless steel PR, B) PUF: Gas velocity 43.37 m h⁻¹ (●) Gas velocity
 4 57.83 m h⁻¹ (○), Gas velocity 77.11 m h⁻¹ (▼), Gas velocity 101.21 m h⁻¹ (△). Values marked
 5 with an arrow indicate the values used for biotic tests.

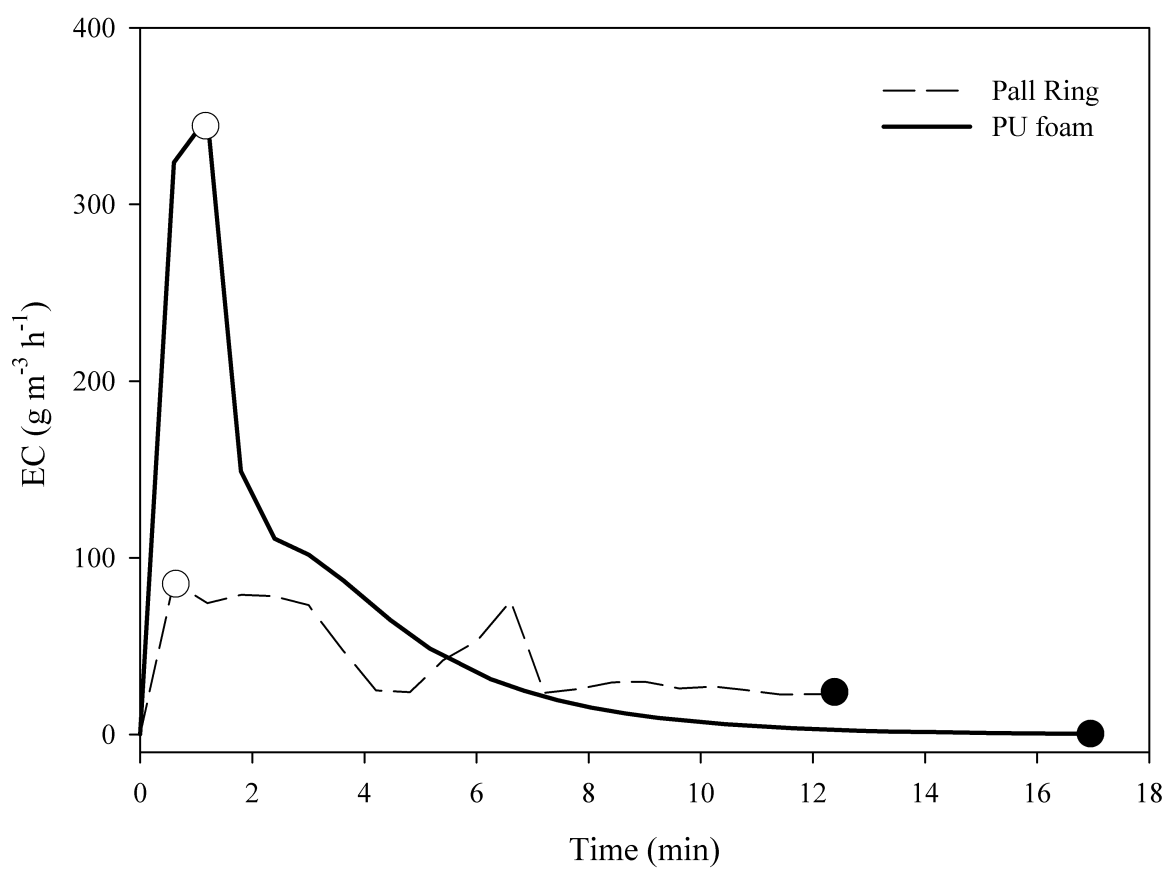
6



1

2 **Fig. 4.** Experimental results and predicted profiles of the HR model obtained from the
 3 respirometric assays with a gas pulse of 10 mL of pure H_2S : Gas-experimental (\square), Gas-model
 4 ($--$), Liquid-experimental (\blacksquare), Liquid-Model ($-$). A) Stainless steel PR, B) PUF.

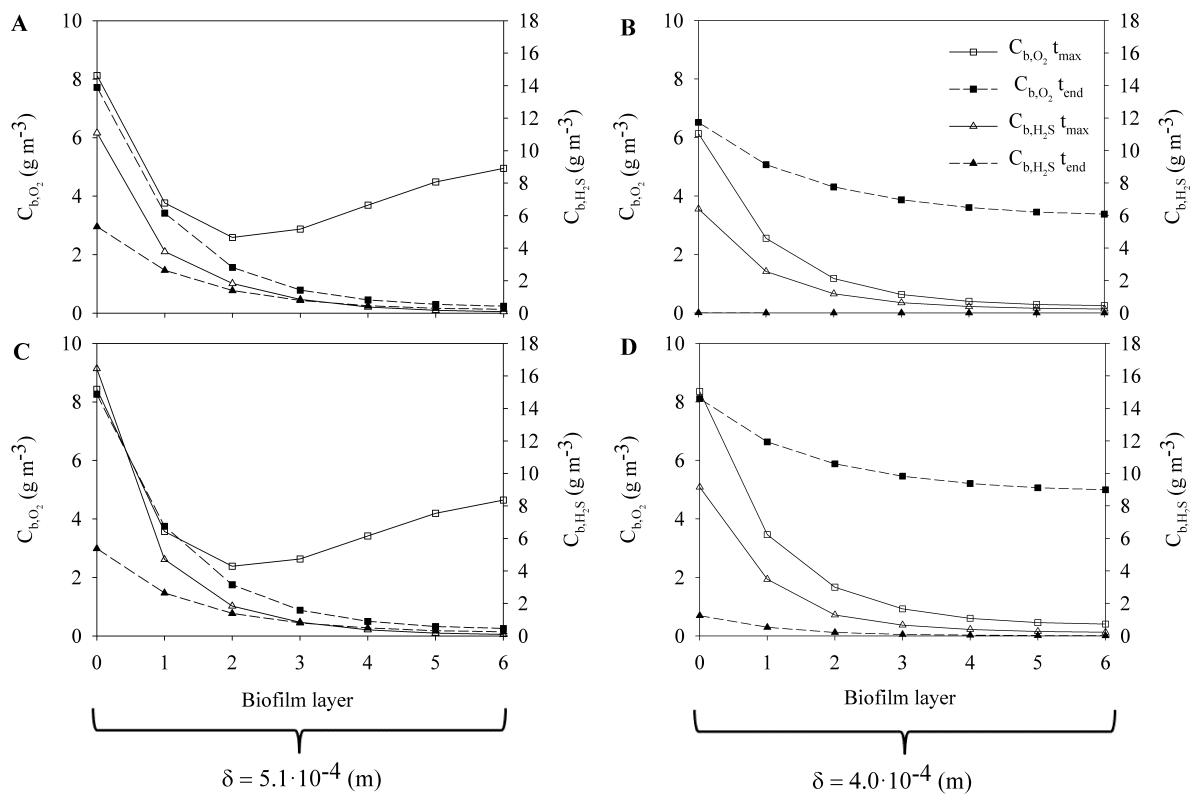
5



1

2 **Fig. 5.** Predicted H₂S elimination capacity for the wetted and non-wetted fractions of colonized
3 PUF and PR packing materials. Circles indicate the time at which the rate controlling step was
4 assessed: t_{max}, (○) and t_{end} (●).

5

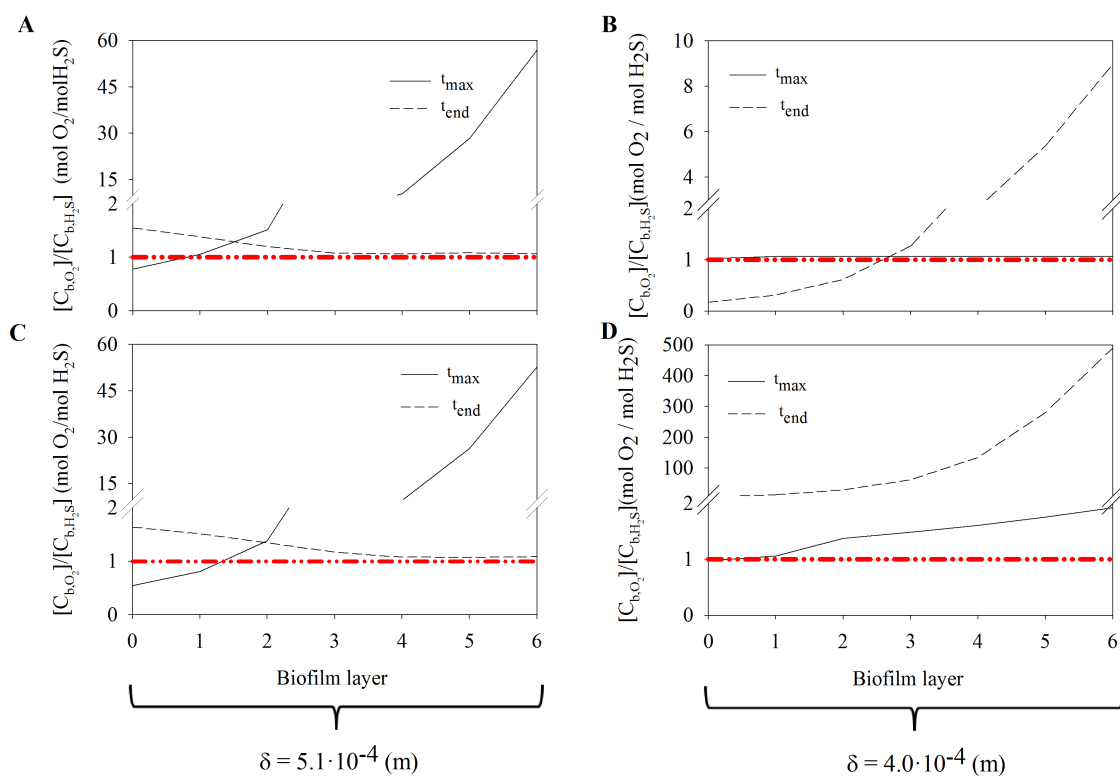


1

2 **Fig. 6.** Simulated dissolved H₂S and oxygen concentration profiles inside the biofilm, at t_{\max} 3 and t_{end} for A) wetted stainless steel PR, B) wetted PUF, C) non-wetted stainless steel PR, and

4 D) non-wetted PUF.

5



1

2 **Fig. 7.** Dissolved oxygen and H_2S concentrations ratios inside the biofilm at t_{max} and t_{end} for A)

3 wetted stainless steel PR, B) wetted PUF, C) non-wetted stainless steel PR, and D) non-wetted

4 PUF. Dash-dotted lines correspond to the molar ratio at which stoichiometry switches occur.

5

1

Table 1. Parameters included in the mathematical model

Parameter	Colonized Pall Rings		Colonized Polyurethane Foam		Units
	Value	Ref.	Value	Ref.	
ε_g	0.70	E.D.	0.85	E.D.	$\text{m}^3_{\text{gas}} \cdot \text{m}^{-3}_{\text{bed}}$
ε_b	0.06	E.D.	0.21	E.D.	$\text{m}^3_{\text{biofilm}} \cdot \text{m}^{-3}_{\text{bed}}$
ε_l	0.10	E.D.	0.09	E.D.	$\text{m}^3_{\text{liquid}} \cdot \text{m}^{-3}_{\text{bed}}$
ε_s	0.18	M.D.	0.03	M.D.	$\text{m}^3_{\text{liquid}} \cdot \text{m}^{-3}_{\text{bed}}$
α	482.00	M.D.	600.00	M.D.	$\text{m}^2 \cdot \text{m}^{-3}_{\text{bed}}$
K_{S,O_2}	1.47	[19]	1.47	[19]	$\text{g} \cdot \text{m}^{-3}$
$D_{\text{diff } O_2}$	7.10×10^{-6}	ICAS ^a	7.10×10^{-6}	ICAS ^a	$\text{m}^2 \cdot \text{h}^{-1}$
$D_{\text{diff } H_2S}$	6.30×10^{-6}	[31]	6.30×10^{-6}	[31]	$\text{m}^2 \cdot \text{h}^{-1}$
He_{O_2}	32.60	ICAS ^a	32.60	ICAS ^a	
He_{H_2S}	0.41	[16]	0.41	[16]	
$K_{La_{g-l}}$	29.31 ± 2.1	E.D.	22.08 ± 0.9	E.D.	h^{-1}
$V_{g \text{ res}}$	6.30×10^{-4}	E.D.	6.30×10^{-4}	E.D.	m^3
$V_{l \text{ res}}$	1.26×10^{-4}	E.D.	1.26×10^{-4}	E.D.	m^3
V_{bed}	6.10×10^{-4}	E.D.	6.10×10^{-4}	E.D.	m^3
α	0.38	[5]	0.36	[5]	$\text{m}^2_{\text{liquid}} \cdot \text{m}^{-2}_{\text{bed}}$
OUR_{end}	6.00	E.D.	7.00	E.D.	$\text{g O}_2 \cdot \text{m}^{-3} \text{ biomass} \cdot \text{h}^{-1}$

^aICAS 13 data base, Denmark.

E.D. Experimental determination.

M.D. Manufacturer data

2

1

2 **Table 2** Fitted parameters for the calibration of the HR mathematical model to the respective

3 PR and PUF assays and other relevant parameters computed.

Parameter	Colonized Pall	Colonized	Units
	Rings	Polyurethane Foam	
OUR_{max} (best fitted)	16237.0	27202.4	$\text{g O}_2 \text{ m}^{-3} \text{ biomass h}^{-1}$
δ (best fitted)	5.1×10^{-4}	4.0×10^{-4}	m
K_{S, H_2S} (best fitted)	9.9	9.9	g m^{-3}
K_i (best fitted)	69.7	69.5	g m^{-3}
EC_{max}	85.7	349.4	$\text{g H}_2\text{S m}^{-3} \text{ h}^{-1}$
β	0.2	0.8	$\text{m}^2 \text{ bio m}^{-2} \text{ bed}$
$q_{O_2 max}$	23.0	38.55	$\text{mmol O}_2 (\text{g biomass min})^{-1}$
a_{t-b}	44.7	180.0	$\text{m}^2 \text{ wetted biofilm m}^{-3} \text{ bed}$
a_{g-b}	72.9	320.0	$\text{m}^2 \text{ non-wetted biofilm m}^{-3}$ bed

4

5

6